Asian Journal of Mycology 8(2): 102–111 (2025) ISSN 2651-1339
www.asianjournalofmycology.org
Article
Doi 10.5943/ajom/8/2/8

A novel non-haired Hyaloscyphaceae species, *Isthmosporiella glabra* sp. nov., in Yunnan Province, China

Li CJY[1,2,3], Zhao Q[3], Hyde KD[2,3], Yu FM[3], Chethana KWT[2*] and Eungwanichayapant PD[1*]

[1]*School of Science, Mae Fah Luang University, Chiang Rai, 57100, Thailand*
[2]*Center of Excellence in Fungal Research, Mae Fah Luang University, Chiang Rai, 57100, Thailand*
[3]*State Key Laboratory of Phytochemistry and Natural Medicines, Kunming Institute of Botany, Chinese Academy of Sciences, Kunming, Yunnan 650201, China*

Li CJY, Zhao Q, Hyde KD, Yu FM, Chethana KWT, Eungwanichayapant PD. 2025 – A novel non-haired Hyaloscyphaceae species, *Isthmosporiella glabra* sp. nov., in Yunnan Province, China. Asian Journal of Mycology 8(2), 102–111, Doi 10.5943/ajom/8/2/8

Abstract

During a survey of discomycetes in Yunnan, China, one saprobic species of *Isthmosporiella* was discovered on decayed wood. It is characterized by tiny glabrous and subsessile apothecia, semi-transparent grayish-yellow (fresh) to dark yellow (dried) discs, *textura globulosa* to *angularis* cells at the medullary excipulum, *textura epidermoidea* cells at the ectal excipulum, and multi-branched, septate paraphyses, clavate asci with trapezoidal apices, and ovoid-navicular ascospores. *Isthmosporiella glabra* is introduced as a new species based on the examination of morphological characteristics and phylogenetic analyses of the combined LSU-ITS dataset. Furthermore, this marks the first sexual morph and the geographic record of *Isthmosporiella* in China. A comprehensive description, illustration, and phylogenetic analysis are provided here to support its classification.

Keywords – 1 new species – Helotiales – one new taxon – phylogeny – sexual morph – taxonomy

Introduction

Hyaloscyphaceae Nannf. was described by Nannfeldt (1932), with three tribes and 13 genera primarily distinguished by the shape and the structure of excipular cells. The generic delimitation of Hyaloscyphaceae has long been controversial and ambiguous, stemming from varying emphasis on morphological features (Hosoya & Otani 1997a, b, Han et al. 2014, Quijada et al. 2017, Kosonen et al. 2021). Subsequently, Arachnopezizeae and Lachneae were reclassified to the family level from Hyaloscyphaceae based on the presence of subiculum surrounding the apothecia, as well as distinct characteristics such as lanceolate paraphyses and multi-septate, granulate hairs. This reclassification was later confirmed by molecular analyses (Han et al. 2014, Kosonen et al. 2021). Recent research has focused on categorizing Hyaloscyphaceae *sensu stricto*, leaving other genera requiring further investigation (Hosoya & Otani 1997a, b, Han et al. 2014, Quijada et al. 2017, Kosonen et al. 2021). The sexual morph of Hyaloscyphaceae is characterized by tiny and brightly-coloured apothecia covered with conspicuous, lageniform to conic, glassy or non-glassy hairs around the margin and lower surface, filiform paraphyses, clavate asci with J+ or J-, and oval to short clavate ascospores (Hosoya & Otani 1997a, b, Han et al. 2014, Quijada et al. 2017, Kosonen et al. 2021).

Submitted 26 February 2025, Accepted 30 September 2025, Published 13 November 2025
Corresponding Author: Kandawatte Wedaralalage Thilini Chethana – e-mail – kandawatte.thi@mfu.ac.th;
Prapassorn Damrongkool Eungwanichayapant – e-mail – prapassorn@mfu.ac.th

Hyaloscyphaceae is globally distributed, especially in the temperate zone, and their members primarily exist as saprobes, occasionally parasitizing both living woody and herbaceous substrates (Han et al. 2014), and 29 genera are accommodated in the family (Hyde et al. 2024).

Isthmosporiella Crous was described by Crous et al. (2023) within Hyaloscyphaceae *sensu lato* with *I. africana* Crous as the type species, based on phylogenetic analysis of the LSU phylogeny. Phylogenetically, *Isthmosporiella* is closely related to *Nagrajchalara*, *Hyaloscypha*, and *Eupezizella*, but their morphologies are quite distinct (Crous et al. 2023). The genus differs from its morphologically similar genera *Isthmolongispora* and *Isthmomyces* by disarticulating the conidial chains into single aseptate conidial propagules (Crous et al. 2023). The asexual morphology of *Isthmosporiella* is characterized by hyaline mycelium, reducing conidiophores that form erect, subcylindrical conidiogenous cells with several sympodial, polyblastic denticles, and producing acropetal chains, containing 4 to 8 fusoid-ellipsoid to clavate conidia, linked by a narrow isthmus (Crous et al. 2023). The saprobic life mode of *Isthmosporiella* is reported from dead twigs, and it is sparsely distributed in South Africa (Crous et al. 2023). Currently, only one species has been included in the Index Fungorum (2025), and no sexual morph has been documented.

During a survey of Leotiomycetes diversity in Yunnan, China, two specimens were discovered on fallen and decayed wood and identified as a new species of *Isthmosporiella* based on morphological and phylogenetic analyses, following Chethana et al. (2021). This study provides a comprehensive morphological description, illustration, and a phylogenetic tree for this newly discovered species.

Materials & methods

Sample collection

Two specimens were obtained from the Ailao Mountains, Yunnan, during the field investigations in July 2024. The local ambient temperature is between 21 °C to 28 °C with altitudes of ca. 2,400 m. The sampling method refers to Li et al. (2024b). The dried specimens were deposited at the Herbarium of Cryptogams, Kunming Institute of Botany, Academia Sinica (HKAS). Facesoffungi numbers were retrieved, following Jayasiri et al. (2015), while Index Fungorum numbers were obtained according to the guidelines provided by Index Fungorum (2025). Since some specimens originate from the Greater Mekong region, the relevant information regarding samples from the Greater Mekong region was submitted to the GMS database as noted by Chaiwan et al. (2021).

Morphological studies

Fresh apothecia were captured in the field using a Canon EOS M100 camera (Canon Co. LTD, Japan). Macro-morphological features of dried apothecia were photographed by a Canon EOS 70D(W) digital camera attached to a C-PSN stereomicroscope (Nikon Corporation, Tokyo, Japan). The dried apothecia were manually sliced with razor blades and then observed using a charge-coupled device SC 2000C connected to a Nikon ECLIPSE Ni-U compound microscope (Nikon Corporation, Tokyo, Japan). Vertical sections were used to examine the excipulum and hymenium. Mature apothecia squashed in water were utilized for observing asci, ascospores, and paraphyses. The blue iodine reaction at the ascus apex was studied using Melzer's reagent. All measurements were carried out using the Tarosoft (R) Image Framework software (IFW) and subsequently adjusted in Adobe Photoshop 2020 (Adobe System, USA). The L/W value indicates the length-to-width ratio of asci. The Q value represents the length-to-width ratio of ascospores, while n denotes the count of measured structures, and Q_m signifies the mean value of Q. The colors of apothecia, hymenium, and excipulum were referenced from https://www.colorhexa.com/.

DNA Extraction, PCR Amplification, and Sequencing

Mature fruiting bodies were carefully selected and thoroughly cleaned using sterilized water and 75% alcoholic solution, and then carefully transferred into a sterile 1.5 mL centrifuge tube using sterilized surgical blades. Total genomic DNA was extracted using the Trilief™ Plant Genomic DNA Kit (Tsingke Biological Technology Co., LTD, Beijing, China). The product amplification primers used for each locus were as follows: for the nuclear internal transcribed spacers (ITS), ITS1-F and ITS4 (White et al. 1990, Gardes & Bruns 1993); for the D1/D2 domain of the nuclear large subunit ribosomal RNA (LSU), LR0R and LR5 (Vilgalys & Hester 1990). The total reaction volume of 25 µL consists of 12.5 µL of 2 × Power Taq PCR MasterMix, 7.5 µL of sterile deionized water, 1 µL of each primer (100 µM stock), and 3 µL of DNA template. Amplifications were conducted in a TC-type gene amplifier (LifeECO) (Hangzhou Bori Technology Co., LTD, Hangzhou Province, China). Reactions consist of an initial denaturation step at 94 °C for 5 minutes, followed by 35 cycles of denaturation at 94 °C for 20 seconds, annealing at 53 °C for 30 seconds for LSU and ITS, followed by extension at 72 °C for 45 seconds, and a final extension at 72 °C for 10 minutes. The PCR products were confirmed using electrophoresis on a 1% agarose gel and then stained with TS-GelRed Ver.2 at a concentration of 10,000 times in water (provided by Tsingke Biological Technology Co., LTD, Beijing, China). The successful products were sequenced at Tsingke Biological Technology Co., LTD in Beijing, China.

Sequence assembly and alignment

The forward and reverse sequences were assembled using ContigExpress (Invitrogen, USA) reviewed and modified in BioEdit 7.2.5.0 (Hall 1999). The newly produced sequences were subjected to a BLASTN search at NCBI to search for their homologous sequences (https://blast.ncbi.nlm.nih.gov/Blast.cgi). All related sequences used for phylogenetic analyses were sourced from GenBank, covering 14 genera (*Amicodisca*, *Arbusculina*, *Crucellisporiopsis*, *Eupezizella*, *Haplographium*, *Hyalopeziza*, *Incrupila*, *Mimicoscypha*, *Olla*, *Isthmosporiella*, *Pseudaegerita*, *Pseudoclathrosphaerina*, *Psilocistella*, and *Resinoscypha*) in Hyaloscyphaceae. *Vandijckella johannae* (CBS 143182) was selected as the outgroup taxon (Crous et al. 2023).

The LSU and ITS datasets were aligned separately using the default settings on the MAFFT v. 7 online server (https://mafft.cbrc.jp/alignment/server/) (Katoh et al. 2019) and then further refined manually in BioEdit v. 7.2.5.0. Two datasets were trimmed using the gappyout option in TrimAl v.1.3 (Capella-Gutiérrez et al. 2009). The final dataset was concatenated in the order 'LSU-ITS' using SequenceMatrix 1.7.8 (Vaidya et al. 2011). The online tool ALTER (Alignment Transformation EnviRonment) was utilized to convert the file format from ".fasta" to ".nexus". The sequences newly generated in this study have been submitted to GenBank (Table 1).

Phylogenetic analyses

The IQ-Tree web portal (http://iqtree.cibiv.univie.ac.at/) was utilized to conduct maximum likelihood (ML) analysis. The substitution model options for each locus were automatically assessed based on the provided partition file. Clade support for the ML analysis was determined through a 1,000 replicate SH-aLRT test and the use of the ultrafast bootstrap (UFB) method (Guindon et al. 2010, Hoang et al. 2018). The most appropriate models for each loci segment were selected automatically by the IQ-Tree web portal. The general time-reversible model with a discrete gamma distribution coupled with a proportion of an invariant (GTR + I + G) was selected for LSU, and the symmetric model with a discrete gamma distribution coupled with a proportion of an invariant for ITS as the best model using MrModeltest v.2.3 (Nylander et al. 2008). Bayesian inference (BI) analysis was conducted using MrBayes v. 3.1.2, with the posterior probabilities (PP) assessed through Markov Chain Monte Carlo sampling (MCMC). Four simultaneous Markov chains ran for 2,000,000 generations, with tree sampling every 100th generation. The MCMC analysis started with a randomly selected tree and sampled at intervals of 1,000 generations. Convergence between parallel runs was suggested by an average standard deviation of <0.01 for split frequencies. The first 25% of total trees were excluded as burn-in, while the remaining trees in each analysis were used to estimate the posterior probability (PP) within the majority-rule consensus tree. PP ≥ 0.95 indicates strong support. The phylogenetic tree obtained was visualized using Figtree v. 1.4.0 (Rambaut 2009) and illustrated with Adobe Illustrator 2020 and Adobe Photoshop 2020 (https://www.adobe.com/).

Table 1 Detailed information and corresponding GenBank accession numbers for the taxa utilized in the phylogenetic analyses of this study.

Taxon name	Voucher	Gene accession No.		References
		ITS	LSU	
Amicodisca svrcekii	TK7157	MT231647	–	Kosonen et al. (2021)
Amicodisca virella	SBRH828	MH221521	MH485388	Unpublished
Arbusculina fragmentans†	CCM F-13486	NR_153520	NG_057024	Baschien et al. (2013)
Crucellisporiopsis marquesiae†	CBS:138895	NR_137925	NG_066166	Crous et al. (2014)
Eupezizella aureliella	KUS-F52070	JN033394	JN086697	Han et al. (2014)
Eupezizella britannica	SBRH863	–	MH485391	Unpublished
Haplographium catenatum	CBS:739.68	FJ839622	FJ839657	Crous et al. (2009)
Haplographium catenatum	CBS:196.73	FJ839620	FJ839655	Crous et al. (2009)
Hyalopeziza alni	TK7210	MT231689	–	Kosonen et al. (2021)
Hyaloscypha daedaleae	CBS:120.91	MH018927	OP340026	Fehrer et al. (2019)
Hyaloscypha daedaleae	CBS:121.91	MH018928	OP340025	Fehrer et al. (2019)
Hyaloscypha finlandica†	CBS:444.86	NR_121279	NG_069568	Schoch et al. (2014)
Hyaloscypha fuckelii	CBS:126292	MH863962	MH875420	Vu et al. (2019)
Hyaloscypha gabretae†	CBS:145341	–	NG_081311	Vohník et al. (2022)
Hyaloscypha gabretae	PK-90	MZ520780	MZ520769	Vohník et al. (2022)
Hyaloscypha gabretae	UKA-123	MZ520782	MZ520771	Vohník et al. (2022)
Hyaloscypha gryndleri†	CBS:145337	–	NG_081312	Vohník et al. (2022)
Hyaloscypha herbarum	CBS:126.91	MH018931	OP340030	Vohník et al. (2022)
Hyaloscypha japonensis	CBS:138.59	MH857831	MH869371	Vu et al. (2019)
Hyaloscypha melinii†	CBS 143705	–	NG_068558	Fehrer et al. (2019)
Hyaloscypha spinulosa	CBS:128.51	MH856778	MH868296	Vu et al. (2019)
Hyaloscypha vitreola	CBS:126276	MH863954	MH875413	Vu et al. (2019)
Hyaloscypha vitreola	M39	EU940231	–	Baral et al. (2009)
Hyaloscypha vraolstadiae†	UAMH 10111	–	NG_068557	Fehrer et al. (2019)
Incrupila aspidii	SBRH909	MT040757	OM218632	Unpublished
Isthmosporiella africana	CBS:150064	OR680771	OR717027	Crous et al. (2023)
Isthmosporiella glabra	**HKAS 145637**	**PV256420**	**PV189469**	**This study**
Isthmosporiella glabra	**HKAS 145636**	**PV256421**	**PV189470**	**This study**
Mimicoscypha lacrimiformis	TK7224	MT231701	–	Kosonen et al. (2021)
Mimicoscypha lacrimiformis	SH17/6	MT231702	–	Kosonen et al. (2021)
Mimicoscypha mimica	CBS:126294	MH863964	MH875421	Vu et al. (2019)
Mimicoscypha mimica	CBS:126293	MH863963	–	Vu et al. (2019)
Mimicoscypha mimica	CBS:126306	MH863971	MH875426	Vu et al. (2019)
Mimicoscypha mimica	CBS:126305	MH863970	MH875425	Vu et al. (2019)
Olla millepunctata	TK7167	MT231705	–	Kosonen et al. (2021)
Olla transiens	TK7125	MT231706	–	Kosonen et al. (2021)
Pseudaegerita corticalis	CBS:125642	MH863722	–	Vu et al. (2019)
Pseudaegerita corticalis	ICMP:15324	EF029224	–	Unpublished
Pseudaegerita viridis	ICMP:15542	EF029235	–	Unpublished
Pseudoclathrosphaerina evamariae	CBS:616.97	MH862664	MH874271	Vu et al. (2019)
Pseudoclathrosphaerina spiralis	JAC13712	MK432781	–	Unpublished
Pseudoclathrosphaerina spiralis	ICMP:15523	EF029231	–	Unpublished
Pseudoclathrosphaerina spiralis	JAC13931	OR565294	MK431483	Unpublished
Psilocistella quercina	U.R. 1422	PP910302	–	Unpublished
Psilocistella quercina	U.R. 1437	PP910285	–	Unpublished
Resinoscypha variepilosa	H289	MT231709	–	Kosonen et al. (2021)
Vandijckella johannae†	CBS:143182	NR_172156	NG_075222	Crous et al. (2017)

Notes: The symbol '†' is used to denote type species; Newly generated sequences are in bold font; The symbol '-' indicates that sequence data is unavailable.

Results

Phylogenetic analyses

The combined LSU and ITS dataset comprised 47 isolates representing 33 taxa, with a total of 1,833 aligned nucleotide sites: the LSU region comprising 1,325 bp and the ITS region comprising

508 bp including gaps. The combined alignment comprised 291 parsimony-informative characters, 91 singleton sites, and 1,451 constant characters. The ML and BI analyses yielded a similar topology. The maximum likelihood matrix had 461 distinct alignment patterns with 39.06% undetermined characters or gaps. The best maximum likelihood tree with a final likelihood value of -8108.494 is shown in Fig. 1. The topological structure of phylogenetic trees in this study exhibits certain differences from that of Crous et al. (2023). For instance, *Isthmosporiella* showed a closer relationship with *Hyaloscypha* in the current study, whereas it was closely related to *Eupezizella* in the large-scale phylogenetic analysis of Helotiales by Crous et al. (2023), which was based only on the LSU sequences (Crous et al. 2023). These differences might be attributed to the distinct loci chosen and the variations in the taxon sampling used in the two analyses.

In our study, *Isthmosporiella glabra* is closely related to *I. africana* (CBS 150064) within Hyaloscyphaceae with ML bootstrap supports of 100% in the SH-aLRT test, 100% in the UFB method, and a Bayesian probability of 1.0 (Fig. 1).

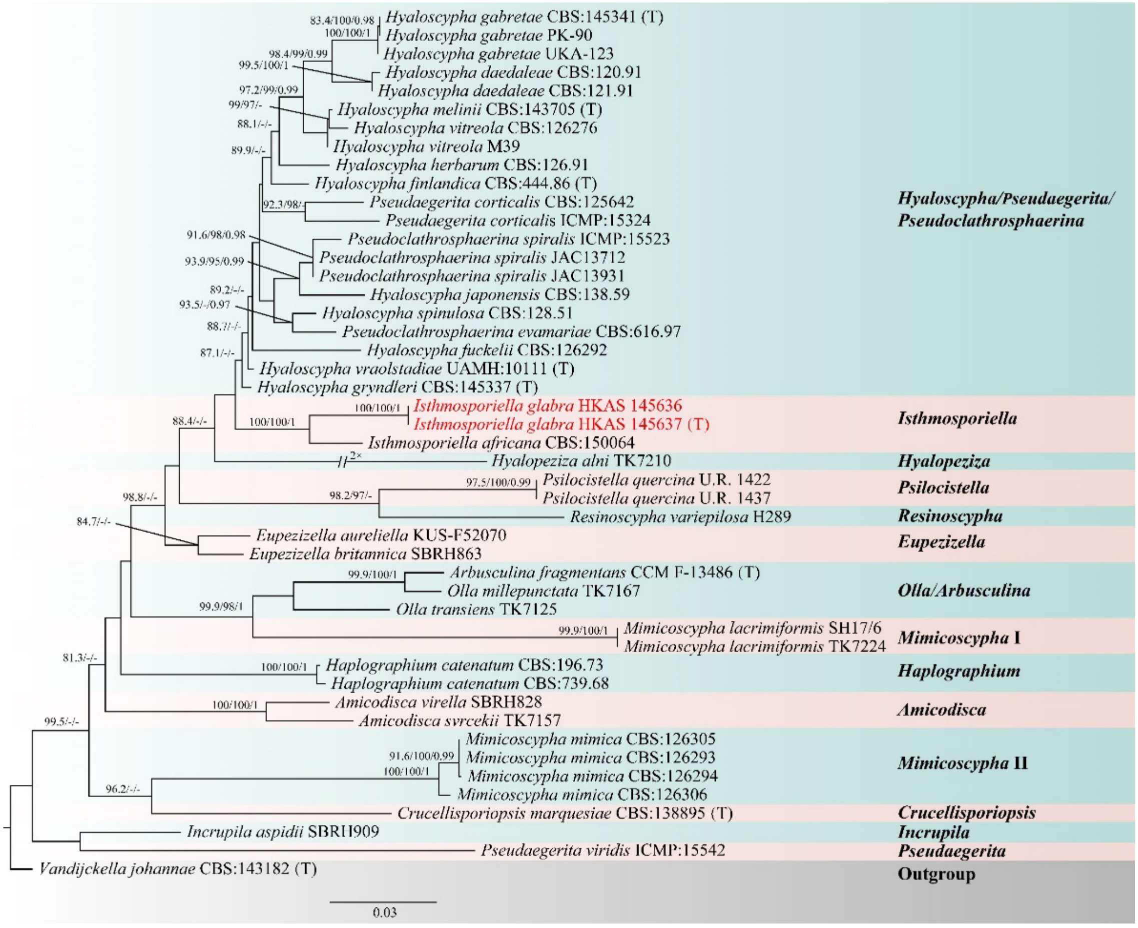

Fig. 1 – Maximum likelihood tree based on the combined LSU and ITS sequences, showing the phylogenetic position of 14 genera in Hyaloscyphaceae. Bootstrap support values for ML ≥ 80 of SH-aLRT or ML > 95 of UFB and posterior probability for BI ≥ 0.90 are indicated above the nodes and separated by "-/-/-" (SH-aLRT/UFB/PP). The newly generated specimens of the current study are in red, whereas the type specimens are denoted as '(T)' following the voucher.

Taxonomy

Isthmosporiella glabra C.J.Y. Li, K.W.T. Chethana, K.D. Hyde & Q. Zhao *sp. nov* Fig 2

Index Fungorum number: IF 902580; Faceoffungi number: FoF 17688

Diagnosis – Apothecia glabrous and subsessile, globose to angular cells of medullary excipulum, epidermoid cells of ectal excipulum, apically J- asci, ovoid-navicular ascospores.

Etymology – The specific epithet refers to the glabrous apothecia, *glabra* (lat.) = glabrous.

Saprobic on the fallen and decayed unidentified wood. Sexual morph: *Apothecia* (0.27–)0.30–0.42(–0.46) mm wide ($\bar{x}$ = 0.36 µm, n = 60) when fresh, 0.12–0.19(–0.27) mm wide ($\bar{x}$ = 0.17 µm, n = 20), 0.12–0.2 µm high ($\bar{x}$ = 0.17 µm, n = 20) when dried, scattered, superficial, discoid, glabrous, and subsessile. *Discs* flat, circular, and semi-transparent grayish-yellow (#747962) when fresh, irregularly circular, dark yellow (#7e774a) to brownish-yellow (#5a4c22) when dried, and the margins smooth, shrink to the center. *Receptacles* smooth and glabrous, pale yellow (#8e956c) when dried, becoming white downwards. *Hymenium* 150–180 µm ($\bar{x}$ = 165 µm, n = 15), hyaline. *Subhymenium* not obvious. *Medullary excipulum* 17–32 µm ($\bar{x}$ = 24 µm, n = 20), comprised of *textura globulosa* to *angularis* cells, (2–)3–8(–12) µm diam. ($\bar{x}$ = 5.4 µm, n = 80), gelatinous, hyaline. *Ectal excipulum* 12–30 µm ($\bar{x}$ = 18 µm, n = 20) and the basal part 25–44 µm ($\bar{x}$ = 33 µm, n = 20) comprised of yellow *textura epidermoidea* cells and hyaline hyphae, the marginal cells elongated. *Paraphyses* 1.2–1.9 µm ($\bar{x}$ = 1.6 µm, n = 50), cylindric to filiform with obtuse apex, hyaline, soft, septate, and branched at the multiple parts, hyaline or very pale. *Asci* 96–126 µm × 10.5–15.5 µm ($\bar{x}$ = 112 × 12.9 µm, n = 40), L/W = 7.0–10.8 ($\bar{x}$ = 8.7 µm, n = 40), 8-spored, unitunicate, clavate with a truncated stipe, rounded corner of a trapezoidal and thicken apex, J- in Melzer's reagent. *Ascospores* 15–21 × 6–8.5 µm ($\bar{x}$ = 18.3 × 7.2 µm, n = 50), Q = (1.9–)2.2–3 µm, Qm = 2.5 ± 0.2 µm, biseriate to overlapping uniseriate, ovoid-navicular, slightly curved, the lower end rounded and the upper end narrower rounded, thin-walled, hyaline, smooth, aseptate, usually with one or two guttules and multiple tiny granulates. Asexual morph: Unknown.

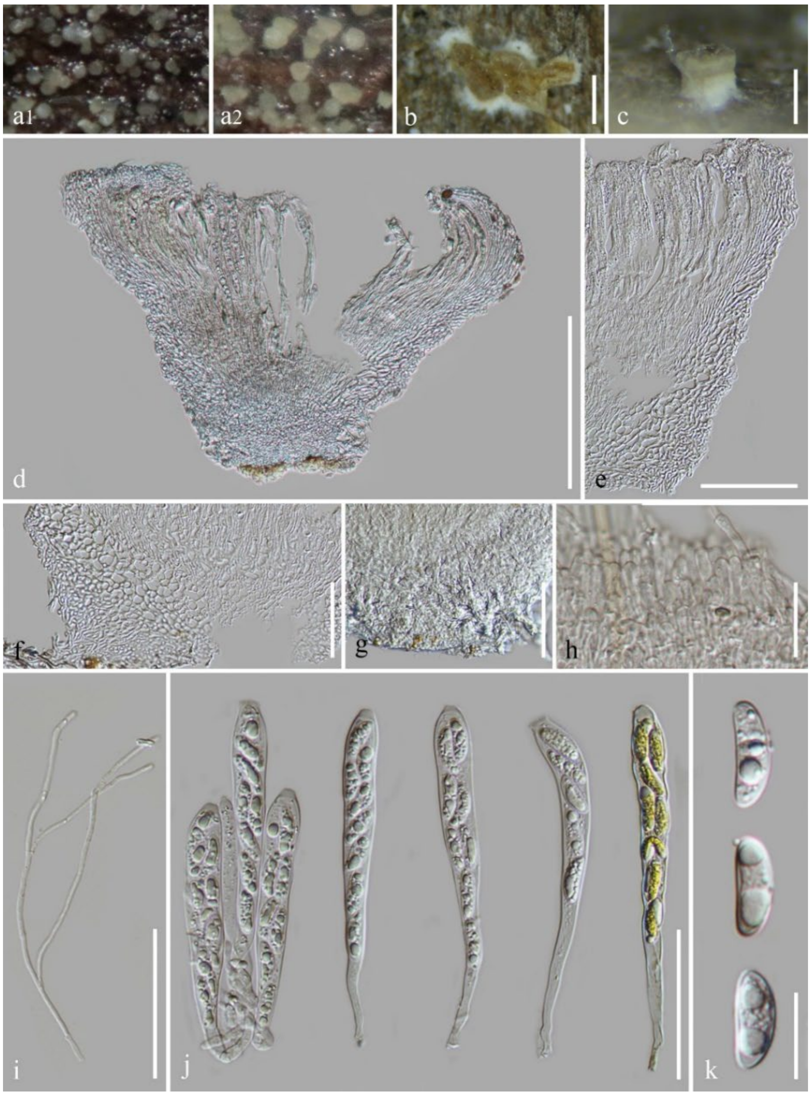

Fig. 2 – *Isthmosporiella glabra* (HKAS 145637, holotype). a1–a2 Fresh apothecia on the decayed branch (a2 the side view of fresh apothecia). b–c Dried apothecia on the substrate. d Vertical section

of an apothecium. e Lateral excipulum. f–g Basal excipulum. h Slightly elongated marginal cells. I Paraphyses. j Asci (the arrow points to the ascus in the Melzer's reagent shows a negative reaction). k Ascospores. Scale bars: b = 400 μm, c = 200 μm, d = 150 μm, e–f, i–j = 50 μm, g = 40 μm, h = 30 μm, k = 15 μm.

Material examined – China, Yunnan Province, Puer City, Jingdong County, altitude 2455 m, on the fallen and decayed unidentified wood, 18 Jul. 2024, Cuijinyi Li, LCJY-1556 (HKAS 145637, holotype); *ibid*., LCJY-1556-2 (HKAS 145638, isotype); *ibid*., 17 Jul. 2024, Cuijinyi Li, LCJY-1551-2 (HKAS 145636, paratype).

Notes – The species can be distinguished from other known taxa of Hyaloscyphaceae by having a glabrous and subsessile apothecium. It is phylogenetically sister to *I. africana* (CBS:150064) with 100%/100%/1.0 (SH-aLRT/UFB/PP). *Isthmosporiella africana* was found to exist as an asexual fungus, but *I. glabra* was only found as a sexual one. At present, these two related species can be distinguished through phylogenetic analysis. *Isthmosporiella glabra* is similar to *Ambrodiscus* species with apically non-amyloid asci but can be distinguished by the cylindrical ascospores surrounded by a gelatinous sheath (Carpenter 1988). *Isthmosporiella glabra* is similar to *Echinula* with multiple-branched paraphyses and slightly curved, ovoid-navicular ascospores, but the latter has obvious setae that are developing from the excipular cells and have J+ asci (Graddon 1977). In addition, *I. glabra* is different from its related genera (*Eupezizella*, *Hyalopeziza* and *Hyaloscypha*) by lacking typical and abundant hair-like structures that originate from the excipular cells (Hosoya & Otani 1997a, b, Quijada et al. 2017).

Discussion

Recent years have witnessed growing interest in studying *Leotiomycetes* in Yunnan Province, China, whose unique climate and diverse ecosystems make it an ideal habitat for these fungi. Researchers have focused on discovering and describing new species and elucidating their ecological roles (Li et al. 2022a, b, 2024a, b, Luo et al. 2024, Su et al. 2022, 2023).

Isthmosporiella was closely related to *Eupezizella* based on the phylogenetic analysis of the LSU dataset (Crous et al. 2023). However, our study revealed a different relationship, showing *Isthmosporiella* as a sister genus to *Hyalopeziza* and *Hyaloscypha*. Our conclusion was based on phylogenetic analyses using two loci (LSU and ITS) and a more focused species sampling within Hyaloscyphaceae, in contrast to the broad taxon sampling based on a single locus (LSU) used in Crous et al. (2023).

Despite the genetic proximity among *Isthmosporiella*, *Hyalopeziza* and *Hyaloscypha*, the latter two genera exhibit distinct morphological differences. *Hyaloscypha* is characterized by its prominent hairs, which are multicellular structures extending from the apothecial surface, and thin-walled prismatic cells in the ectal excipulum (Quijada et al. 2017). *Hyalopeziza* is characterized by its very thick-walled, glassy, straight apothecial hairs. In contrast, *Isthmosporiella* lacks these hair-like structures. Instead, it possesses slightly elongated marginal cells, which, while distinct, do not qualify as true hairs. This morphological distinction differentiates *Isthmosporiella* within the family and suggests that it occupies a unique evolutionary niche (Quijada et al. 2017, Kosonen et al. 2021). The absence of hair-like features, combined with other subtle morphological differences, makes *Isthmosporiella* a morphologically specific genus within Hyaloscyphaceae (Hosoya & Otani 1997a, b, Han et al. 2014, Quijada et al. 2017, Kosonen et al. 2021). However, this trait also raises questions about its taxonomic significance. While this character appears to be a defining trait, confirming its taxonomic reliability requires further research, particularly through increased sampling and the discovery of sexual morphs. The limited availability of molecular data for many taxa within Hyaloscyphaceae has led to ongoing controversy regarding the phylogenetic placement of genera, including *Isthmosporiella* and *Hyaloscypha*.

Taxonomic studies in Hyaloscyphaceae have been complicated due to morphological plasticity, lack of gene data such as protein-coding genes, and incomplete sampling of cryptic species. Resolving the systematics of this family will require a combination of multi-gene phylogenies, expanded taxon sampling, and detailed morphological analyses. These approaches are critical for gaining a better understanding of the evolution and ecological roles of genera such as *Isthmosporiella* and *Hyaloscypha* within Hyaloscyphaceae.

Acknowledgements

This study is supported by the Second Tibetan Plateau Scientific Expedition and Research Program (Grant No. 2024QZKK02010303) and the Yunnan Revitalization Talent Support Program: Science & Technology Champion Project (202305AB350004). Feng-Ming Yu thanks to the Postdoctoral Fellowship Program of China Postdoctoral Science Foundation under Grant Number GZB20240769. The authors would like to thank Dr. Shaun Pennycook for his valuable assistance with the Latin binomial. Cui-Jin-Yi Li would like to thank Mae Fah Luang University for the tuition fee grant (GR-ST-PS-63-03) for the doctoral degree program and the dissertation writing grant (Grant No. อว7702(6)/143(no.0438)).

References

Baral HO, De Sloover JR, Huhtinen S, Laukka T et al. 2009 – An emendation of the genus *Hyaloscypha* to include *Fuscoscypha* (Hyaloscyphaceae, Helotiales, Ascomycotina). Karstenia 49, 1–17.

Baschien C, Tsui CKM, Gulis V, Szewzyk U, Marvanová L. 2013 – The molecular phylogeny of aquatic hyphomycetes with affinity to the Leotiomycetes. Fungal biology 117(9), 660–672.

Capella-Gutiérrez S, Silla-Martínez JM, Gabaldón T. 2009 – trimAl: a tool for automated alignment trimming in large-scale phylogenetic analyses. Bioinformatics 25, 1972–1973.

Carpenter SE 1988 – *Ambrodiscus*, a new genus of inoperculate Discomycetes from ambrosia beetle galleries. Mycologia 80, 320–323.

Chaiwan N, Gomdola D, Wang S, Monkai J et al. 2021 – https://gmsmicrofungi. org: an online database providing updated information of microfungi in the Greater Mekong Subregion. Mycosphere 12, 1409–1422.

Chethana TKW, Manawasinghe IS, Hurdeal VG, Bhunjun CS et al. 2021 – What are fungal species and how to delineate them? Fungal Diversity 109, 1–25.

Crous PW, Braun U, Wingfield MJ, Wood AR. et al. 2009 – Phylogeny and taxonomy of obscure genera of microfungi. Persoonia: Molecular Phylogeny and Evolution of Fungi 22, 139–161.

Crous PW, Wingfield MJ, Schumacher RK, Summerell BA et al. 2014 – Fungal Planet description sheets: 281–319. Persoonia-Molecular Phylogeny and Evolution of Fungi 33(1), 212–289.

Crous PW, Wingfield MJ, Burgess TI, Carnegie AJ et al. 2017 – Fungal Planet description sheets: 625–715. Persoonia: Molecular Phylogeny and Evolution of Fungi 39, 270–467.

Crous PW, Costa M, Kandemir H, Vermaas M et al. 2023 – Fungal Planet description sheets: 1550–1613. Persoonia: Molecular Phylogeny and Evolution of Fungi 51, 280–417.

Fehrer J, Réblová M, Bambasová V, Vohník M. 2019 – The root-symbiotic *Rhizoscyphus ericae* aggregate and *Hyaloscypha* (Leotiomycetes) are congeneric: Phylogenetic and experimental evidence. Studies in Mycology 92, 195–225.

Gardes M, Bruns T. 1993 – ITS primers with enhanced specificity for basidiomycetes-application to the identification of mycorrhizae and rusts. Molecular ecology 2, 113–118.

Graddon W. 1977 – Some new discomycete species: 4. Transactions of the British Mycological Society 69, 255–273.

Guindon S, Dufayard J-F, Lefort V, Anisimova M et al. 2010 – New algorithms and methods to estimate maximum-likelihood phylogenies: assessing the performance of PhyML 3.0. Systematic Biology 59, 307–321.

Hall T. 1999 – BioEdit: a user-friendly biological sequence alignment editor and analysis program for Windows 95/98/NT. Nucleic Acids Symposium Series 41, 95–98.

Han JG, Hosoya T, Sung GH, Shin HD. 2014 – Phylogenetic reassessment of Hyaloscyphaceae *sensu lato* (Helotiales, Leotiomycetes) based on multi-gene analyses. Fungal Biology 118, 150–167.

Hoang DT, Chernomor O, Von Haeseler A, Minh BQ, Vinh LS. 2018 – UFBoot2: improving the ultrafast bootstrap approximation. Molecular Biology and Evolution 35, 518–522.
Hosoya T, Otani Y. 1997a – Hyaloscyphaceae in Japan (1): Non-glassy-haired members of the tribe Hyaloscypheae. Mycoscience 38, 171–186.
Hosoya T, Otani Y. 1997b – Hyaloscyphaceae in Japan (2): Glassy-haired members of the tribe Hyaloscypheae. Mycoscience 38, 187–205.
Hyde KD, Noorabadi MT, Thiyagaraja V, Mq H et al. 2024 – The 2024 Outline of Fungi and fungus-like taxa. Mycosphere 15(1), 5146–6239.
Index Fungorum. 2025 – Index Fungorum. Available at: http://www.indexfungorum.org/ (Accessed on February 13, 2025)
Jayasiri SC, Hyde KD, Ariyawansa HA, Bhat J et al. 2015 – The Faces of Fungi database: fungal names linked with morphology, phylogeny and human impacts. Fungal Diversity 74, 3–18.
Katoh K, Rozewicki J, Yamada KD. 2019 – MAFFT online service: multiple sequence alignment, interactive sequence choice and visualization. Briefings in Bioinformatics 20, 1160–1166.
Kosonen T, Huhtinen S, Hansen K. 2021 – Taxonomy and systematics of Hyaloscyphaceae and Arachnopezizaceae. Persoonia-Molecular Phylogeny and Evolution of Fungi 46, 26–62.
Li CJY, Chethana KWT, Hyde KD, Zhao Q. 2022a – Phylogeny and morphology reveal a new species of *Chlorociboria* (Chlorociboriaceae, Leotiomycetes) from southwestern China. Phytotaxa 554, 122–134.
Li CJY, Chethana KWT, Lu ZY, Zhao Q. 2022b – Two novel species of Lachnaceae (Helotiales, Leotiomycetes) from southwestern China. Current Research in Environmental & Applied Mycology (Journal of Fungal Biology) 12, 333–345.
Li CJY, Chethana KWT, Eungwanichayapant PD, Zhou DQ, Zhao Q. 2024a – Additional four species of *Tatraea* (Leotiomycetes, Helotiales) in Yunnan Province, China. MycoKeys 102, 127–154.
Li CJY, Chethana KWT, Eungwanichayapant PD, Luo L et al. 2024b – *Longistipes* gen. nov. and four novel species of Hyphodiscaceae along with six new collections of Leotiomycetes in Yunnan Province, China. Mycosphere 15, 4744–4787.
Luo L, Wei D, Zhao Q, Chethana KWT. 2024 – Unveiling the diversity: A novel species of *Dicephalospora* (Helotiaceae, Helotiales) discovered in China. Phytotaxa 652, 59–68.
Nannfeldt JA. 1932 – Studien uber die morphologie und systematik der nicht-lichenisierten inoperculaten Discomyceten. Nova Acta Regiae Societatis Scientiarum Upsaliensis, Series IV 8, 1–368.
Nylander J, Zoology S, Posada D, Mrmodeltest R, Os F. 2008 – MrModeltest2 v. 2.3 (Program for selecting DNA substitution models using PAUP*) Evolutionary Biology Centre. Uppsala, Sweden.
Quijada L, Huhtinen S, Negrín R, Beltrán-Tejera E. 2017 – Studies in Hyaloscyphaceae associated with major vegetation types in the Canary Islands II: a revision of *Hyaloscypha*. Willdenowia 47, 31–42.
Rambaut A. 2009 – FigTree. Tree figure drawing tool. Available at: http://tree.bio.ed.ac.uk /software/figtree/. (v. 1.4.0)
Schoch CL., Robbertse B, Robert V, Vu D et al. 2014 – Finding needles in haystacks: linking scientific names, reference specimens and molecular data for Fungi. Database 2014, bau061.
Su HL, Chethana KWT, Li L, Li W, Zhao Q. 2022 – *Diplocarpa constans* sp. nov., a new species of Cordieritidaceae from Yunnan, China. Phytotaxa 561, 75–84.
Su HL, Chethana KWT, Zeng M, Zhao Q. 2023 – Two new species of *Erioscyphella* (Lachnaceae) from southwestern. Current Research in Environmental & Applied Mycology (Journal of Fungal Biology) 13, 16–33.
Vaidya G, Lohman DJ, Meier R. 2011 – SequenceMatrix: concatenation software for the fast assembly of multi-gene datasets with character set and codon information. Cladistics 27, 171–180.
Vilgalys R, Hester M. 1990 – Rapid genetic identification and mapping of enzymatically amplified ribosomal DNA from several *Cryptococcus* species. Journal of Bacteriology 172, 4238–4246.

Vohník M, Figura T, Réblová M. 2022 – *Hyaloscypha gabretae* and *Hyaloscypha gryndleri* spp. nov. (Hyaloscyphaceae, Helotiales), two new mycobionts colonizing conifer, ericaceous and orchid roots. Mycorrhiza 32, 105–122.

Vu D, Groenewald M, De Vries M, Gehrmann T et al. 2019 – Large-scale generation and analysis of filamentous fungal DNA barcodes boosts coverage for kingdom fungi and reveals thresholds for fungal species and higher taxon delimitation. Studies in Mycology 92, 135–154.

White TJ, Bruns T, Lee SJWT, Taylor J. 1990 – Amplification and direct sequencing of fungal ribosomal RNA genes for phylogenetics. PCR protocols: a guide to methods and applications 18, 315–322.